HHS Public Access

Author manuscript

Acta Neuropathol. Author manuscript; available in PMC 2017 January 01.

Published in final edited form as:

Acta Neuropathol. 2016 January ; 131(1): 103–114. doi:10.1007/s00401-015-1514-0.

Prion-like propagation of mutant SOD1 misfolding and motor neuron disease spread along neuroanatomical pathways

Jacob I. Ayers[1], **Susan E. Fromholt**[1], **Veronica M. O'Neal**[1], **Jeffrey H. Diamond**[1], and **David R. Borchelt**[1,2]

Jacob I. Ayers: jayers.123ja@ufl.edu

[1]Department of Neuroscience, Center for Translational Research in Neurodegenerative Disease (CTRND), University of Florida, Box 100159, Gainesville, FL 32610, USA

[2]SantaFe HealthCare Alzheimer's Disease Research Center, McKnight Brain Institute, University of Florida, Gainesville, FL 32610, USA

Abstract

A hallmark feature of amyotrophic lateral sclerosis (ALS) is that symptoms appear to spread along neuroanatomical pathways to engulf the motor nervous system, suggesting a propagative toxic entity could be involved in disease pathogenesis. Evidence for such a propagative entity emerged recently in studies using mice that express G85R-SOD1 mutant protein fused to YFP (G85R-SOD1: YFP). Heterozygous G85R-SOD1:YFP transgenic mice do not develop ALS symptoms out to 20 months of age. However, when newborns are injected with spinal homogenates from paralyzed mutant SOD1 mice, the G85R-SOD1:YFP mice develop paralysis as early as 6 months of age. We now demonstrate that injecting spinal homogenates from paralyzed mutant SOD1 mice into the sciatic nerves of adult G85R-SOD1:YFP mice produces a spreading motor neuron disease within 3.0 ± 0.2 months of injection. The formation of G85R-SOD1:YFP inclusion pathology spreads slowly in this model system; first appearing in the ipsilateral DRG, then lumbar spinal cord, before spreading rostrally up to the cervical cord by the time mice develop paralysis. Reactive astrogliosis mirrors the spread of inclusion pathology and motor neuron loss is most severe in lumbar cord. G85R-SOD1:YFP inclusion pathology quickly spreads to discrete neurons in the brainstem and midbrain that are synaptically connected to spinal neurons, suggesting a trans-synaptic propagation of misfolded protein. Taken together, the data presented here describe the first animal model that recapitulates the spreading phenotype observed in patients with ALS, and implicates the propagation of misfolded protein as a potential mechanism for the spreading of motor neuron disease.

Correspondence to: Jacob I. Ayers, jayers.123ja@ufl.edu.

Electronic supplementary material The online version of this article (doi:10.1007/s00401-015-1514-0) contains supplementary material, which is available to authorized users.

Compliance with ethical standards

Conflict of interest The authors declare they have no competing interests.

Keywords

Superoxide dismutase 1; Amyotrophic lateral sclerosis; Transmissibility; Seeding; Motor neuron disease

Introduction

ALS is a fatal, neurodegenerative disease, in which the progressive degeneration of upper and lower motor neurons results in muscle atrophy, paralysis, and ultimately death. Although it has been studied extensively for the better part of the last half-century, the disease still has only one therapeutic option that is only modestly effective. Approximately 10 % of all ALS cases have a familial etiology (fALS), and mutations in superoxide dismutase-1 (*SOD1*) were the first to be identified as causative [22]. There are now more than 170 mutations identified as causative in the SOD1 gene (http://alsod.iop.kcl.ac.uk/). It is thought that all of these mutations cause the protein to gain a toxic property that is, by some means, associated with increased propensity for the protein to adopt aberrantly folded, detergent-insoluble conformations [4, 6, 12, 19, 29]. Importantly, the symptoms of ALS in SOD1-linked cases are very similar to those observed in sporadic cases of ALS (sALS). In both sporadic and SOD1-linked ALS, muscle weakness and paralysis begin focally before appearing to spread to anatomically adjacent muscle groups. The rate at which symptoms spread from one motor complex to another until reaching the respiratory motor complex dictates how long patients will live with the disease. Recent reports have suggested that a prion-like mechanism of spread could be involved in ALS, based upon correlations made from neuropathological findings and clinical symptoms observed in patients [5, 20, 21]. It is well established that misfolded prion proteins can spread along anatomical pathways [14], and that proteins such as α-synuclein and tau mediate anatomical spreading of a misfolded conformation [7, 14, 18, 23–25, 30]. However, none of these proteins have been implicated in motor neuron disease, leaving the identity of the spreading entity unresolved.

Recently, a number of studies have revealed the ability for SOD1 to undergo prion-like seeded aggregation. Although the majority of these studies have involved cell culture models, they have demonstrated the ability for misfolded forms of SOD1, including the wild-type (WT) variant, to move from cell-to-cell via various mechanisms and propagate aggregation [10, 17]. We recently demonstrated a working model for motor neuron disease transmission by injecting spinal homogenates from paralyzed G93A SOD1 mice into the spinal cords of newborn transgenic mice expressing the G85R-SOD1 mutant fused to YFP (G85R-SOD1:YFP) [1]. The G85R-SOD1:YFP mice are extremely useful in visualizing mutant SOD1 misfolding; mice homozygous for this transgene develop typical symptoms of motor neuron disease [28]. In the spinal cords of paralyzed, homozygous, G85R-SOD1:YFP mice, the fusion protein changes distribution from that of a diffusely distributed protein to inclusion-like structures [28]. This transformation in distribution is accompanied by biochemical evidence that the fusion protein forms detergent-insoluble aggregates [28]. In our transmission paradigm, we use mice that are heterozygous for the transgene and lack both phenotypic symptoms of motor neuron disease and pathologic evidence of G85R-SOD1:YFP inclusion formation [28]. For reasons that have yet to be elucidated, G85R-

SOD1:YFP mice were uniquely permissive for the induction of motor neuron disease when we injected spinal homogenates from paralyzed G93A mice into the spinal cords of newborn G85R-SOD1:YFP mice [1]. Pathologically, these induced mice develop G85R-SOD1:YFP inclusions throughout the spinal cord and brainstem. Moreover, similar to the host adaptation phenomenon observed upon the serial passage and isolation of prion strains, upon second passage of homogenate from these paralyzed G85R-SOD1: YFP mice (G93A → G85R-SOD1:YFP) back into naïve G85R-SOD1-YFP mice, we observed an increased attack rate and decreased incubation period. These latter observations are consistent with the notion that misfolded SOD1 can penetrate cellular membranes and can act as template in directing the misfolding of naïve SOD1 molecules to propagate disease. Based on these prion-like features, and the lack of evidence of transmission to non-transgenic mice or mice that expressed untagged mutant SOD1, we advocated that mutant SOD1 be considered a pseudoprion [1].

In the present study, we have used this permissive G85R-SOD1:YFP model in a paradigm of adult sciatic nerve injection, first used in the study of prion trans-synaptic transmission [2, 3], to produce a new model of spreading motor neuron disease. We show that a single unilateral injection of minute quantities of spinal homogenates from paralyzed G85R-SOD1:YFP mice efficiently induces a progressive motor neuron disease that spreads from the limb of injection to engulf the spinal axis. The spread of disease in the spinal cord is evident in the distribution of G85R-SOD1: YFP inclusion pathology, which first takes hold in neurons innervating the injected limb before appearing more rostrally as the mice develop symptoms. Similarly, astrogliosis first appears in lumbar cord before spreading rostrally to thoracic and cervical regions. Additionally, we observed rapid spread of pathology to brain structures that innervate the cord, indicating the potential for transsynaptic spread of misfolded mutant SOD1. This new model provides the first platform in which the focal origin of the disease process can be manipulated; a model that should enable more definitive assessments of therapeutics designed to slow disease progression.

Methods

Mice

All studies involving mice were approved by the Institutional Animal Care and Use Committee (IACUC) at the University of Florida in accordance with NIH guidelines. All animals were housed one to five to a cage and maintained on ad libitum food and water with a 12 h light/dark cycle. The G85R-SOD1:YFP mice have been described previously [28] and were maintained on the FVB/NJ background.

Inoculum preparation

Homogenates to produce inoculum were prepared as previously described [1]. Briefly, spinal cords from either asymptomatic, heterozygous, G85R-SOD1:YFP mice or G85R-SOD1:YFP mice that had become paralyzed after injection with homogenate from a paralyzed G93A mouse (G93A → G85R-SOD1:YFP) were homogenized in PBS to produce a 10 % homogenate (w/v), containing 1:100 v/v protease inhibitor cocktail (Sigma, St.

Louis, MO) by sonication 4 times for 20 s each. Homogenates were then clarified by a low-speed spin at ~800×*g* for 10 min and the supernatants were aliquoted and placed at −80 °C.

Animal inoculations

Sciatic nerve injections of spinal cord homogenates were performed on female FVB mice expressing the G85R-SOD1: YFP transgene, as previously described [1]. Female mice were used because male mice in this strain are particularly aggressive, and fighting among siblings can lead to injuries severe enough to require the removal of animals from the study. Prior to the injection, mice were injected with Meloxicam (2 mg/kg) (Norbrook, Overland Park, KS), to relieve pain, and the injection site was shaved and sterilized. The mice were then deeply anesthetized with isoflurane using a precision vaporizer machine with gas scavenging system attached and a small incision was then made in the skin of the hind limb and the sciatic nerve was exposed at the popliteal fossa. A 33-gauge needle containing the inoculum was inserted in the sciatic nerve and reciprocated 10 times, which has been shown to greatly enhance the efficiency of prion transport to the spinal cord [3]. 2 μl of prepared homogenate was injected under the perineurium of the sciatic nerve and the incision was then closed with stainless steel clips and cleaned. Following surgery, 2 mg/kg Meloxicam was administered at 24 and 48 h post-surgery.

Behavioral assessment

Once a week following injections, mice were assessed for hind limb impairments. The mice were held by the tail and each of their hind feet was positioned next to the lip of their cage to allow them to grip the edge. The tails of the mice were then lifted up to determine their hind limb strength in the ipsilateral versus contralateral limb. The strength was then determined by the following criteria: (1) weakening grip strength, (2) no grip strength, but still able to move limb and freely move around the cage, and (3) no grip strength, very little movement of limb, and difficulty moving around the cage. The endpoint for these experiments was the point at which both hind limbs were paralyzed or at a point in which the animals displayed difficulties obtaining food and water.

Tissue collection

Mice were anesthetized with isoflurane and perfused transcardially with 20 ml of PBS followed by 20 ml of 4 % paraformaldehyde. The spinal cords, brains, both sciatic nerves, both gastrocnemius muscles, and the L3, L4, and L5 dorsal root ganglia (DRGs) were immediately removed and placed in 4 % paraformaldehyde for 24–48 h at 4 °C prior to paraffin processing.

Fluorescence microscopy

All tissues were embedded in paraffin, cut at 7–10 μm and placed onto slides. For direct YFP fluorescence within the tissue, sections were deparaffinized and cover-slipped in mounting media containing DAPI (Vector, Bulingame, CA). For glial-fibrillary acidic protein (GFAP) analysis, sections were deparaffinized, blocked in normal serum, and incubated with a rabbit anti-GFAP antibody (Dako Carpinteria, CA) overnight at 4 °C. The slides were then incubated for 30 min with an anti-rabbit alexa fluor 568 secondary antibody

(Invitrogen, Carlsbad, CA) and then cover-slipped in mounting media containing DAPI. Fluorescence images were either visualized on an epifluorescence Olympus BX60 microscope or imaged using the Scanscope FL image scanner (Aperio Technologies, Buffalo Grove, IL) and images of representative areas were taken using the ImageScope software (Aperio Technologies, v.12.1.0.5029).

Quantification of G85R-SOD1:YFP inclusions and GFAP immunoreactivity

Spinal cords from the injected animals were arranged in the paraffin blocks so that each paraffin section from a single animal contained two cervical segments, three thoracic segments, and two lumbar segments. Fluorescent images were captured using the Scanscope FL scanner as described above for two paraffin sections per animal with at least three animals per timepoint being analyzed. Using ImageJ, each section of spinal cord was thresholded to highlight the features to be quantified and to diminish background signal. The strong fluorescent intensities of the G85R-SOD1:YFP aggregates and robust GFAP immunoreactivity enabled this technique of quantification. For inclusion quantification, objects were carefully inspected to confirm them as pathologic structures, and then the % area of the thresholded aggregates was calculated within each spinal cord section. This value was averaged across sections from similar levels of cord for each animal and for each timepoint. For GFAP quantification, the % area of the thresholded astrocytes was calculated within the gray matter of each spinal cord section and averaged across similar levels of cord for each animal and for each timepoint.

Motor neuron quantification

Motor neurons were first labeled by immunohistochemistry using an anti-choline acetyltransferase (ChAT) antibody. Briefly, spinal cord sections containing 6–8 pieces of spinal cord spanning the entire length of the spinal cord were deparaffinized and processed for antigen retrieval by steaming in sodium citrate buffer (pH 6.0) for 30 min. Following blocking for endogenous peroxidases in 0.3 % H_2O_2 in PBS, sections were blocked in 10 % normal horse serum (Vector Labs, Burlingame, CA) for 30 min, then incubated in anti-ChAT at 1:400 overnight at 4 °C. The sections were then incubated in a horse-anti goat secondary antibody (Vector Labs, Burlingame, CA) at 1:500 for 30 min at room temperature, treated with ABC solution (Vector Labs, Burlingame, CA) for 20 min and developed with DAB substrate (Sigma, St. Louis, MO). The ChAT-positive motor neurons in four spinal cord sections per animal and at least three animals per timepoint were counted by three individuals blind to animal identification and then the numbers were averaged as explained in the figure legend.

Statistical analysis

All statistical analyses were analyzed in GraphPad PRISM 5.01 Software (La Jolla, CA) as explained in figure legends.

Results

Transmissibility of motor neuron disease by sciatic nerve injection

In a recent study, involving only a few mice, we observed the first hint that it might be possible to develop an induced model of ALS in which the focal origin of the disease could be manipulated. We observed that a single G85R-SOD1: YFP animal that received an injection of spinal homogenates from paralyzed G93A SOD1 mice into the sciatic nerve, as an adult, developed motor neuron disease at 2.7 months post-injection [1]. However, most of the G85R-SOD1:YFP mice inoculated by this method did not develop paralysis or focal limb weakness, and these asymptomatic animals were devoid of pathologic inclusions when killed for analysis (data not shown). Thus, although the outcome was intriguing, a model with such poor reliability would be difficult to use in studying the spread of motor neuron disease.

To determine whether a more reliable and useful model could be generated, we built upon the observation that transmission frequency of motor neuron disease in our newborn intra-spinal inoculation model is dramatically increased with second passage homogenates [1]. In practical terms this means that first passage injections of spinal homogenates from paralyzed G93A SOD1 mice into newborn G85R-SOD1:YFP mice produces disease at a 50 % attack rate (half the mice remain disease free). When spinal homogenates are then made from the paralyzed first passage mice (G93A → G85R-SOD1:YFP) and used for injection into the spinal cords of newborn G85R-SOD1:YFP mice, then the attack rate rises to 100 % and the age to onset of symptoms is reduced [1]. Accordingly, when we injected 10 % spinal homogenates from paralyzed G93A → G85R-SOD1:YFP mice, unilaterally into the sciatic nerves of 2–3-month-old G85R-SOD1: YFP mice, we observed that eight of the ten animals developed end-stage paralysis by 3.0 ± 0.2 months post-injection (p.i.) (Table 1). In all of these animals, the first limb to show weakness was the ipsilateral limb (Fig. 1). Based on qualitative observations, the ipsilateral hind limb became paralyzed before the contralateral hind limb began to display noticeable weakness (Fig. 1). As negative controls, we injected the sciatic nerve with either PBS or 10 % spinal homogenates from an asymptomatic heterozygous G85R-SOD1:YFP mouse. The mice injected with these control preparations were harvested at 12.6 and 8.5 months p.i., respectively, and displayed no signs of MND (Table 1) or G85R-SOD1:YFP inclusion pathology (Fig. 2). Thus, with this paradigm, we establish a relatively reproducible model of induced motor neuron disease in which the origin of disease is defined by injecting spinal homogenates into a single sciatic nerve. The paralysis induced from this injection paradigm appears to spread from the ipsilateral limb to the contralateral limb, mirroring the spread of symptoms observed in ALS.

Evolution of G85R-SOD1:YFP inclusion formation following sciatic nerve injection

To better understand the spread of pathology over time, we injected G85R-SOD1:YFP mice unilaterally within the sciatic nerve with the same homogenate as described above, and sacrificed the animals at 1 and 2 months p.i. At 1 month p.i. the mice had no observable phenotype, and when we analyzed their spinal cords, the distribution of G85R-SOD1:YFP inclusion pathology was limited. In the ipsilateral L3–L5 dorsal root ganglia (DRG), which are associated with the ipsilateral sciatic nerve, we detected limited inclusion pathology

(Fig. 3a). No inclusions were observed in the contralateral DRG (Fig. 3b) and no G85R-SOD1: YFP inclusions could be identified in the spinal cord (Fig. 4a–c). By 2 months post-injection, a subset of the injected animals began to show ipsilateral hind limb weakness, while other animals remained asymptomatic. The mice that were asymptomatic had a higher frequency of G85R-SOD1:YFP inclusions within the ipsilateral DRG than the 1 month cohort, and also began to develop inclusions in the contralateral DRG, albeit much less abundant than the ipsilateral DRG and most often observed in the nerve (Fig. 3c, d). These animals also displayed inclusions within their spinal cords, with numerous punctate aggregates appearing within neurons and the neuropil in the ipsilateral lumbar spinal cord (dorsal and ventral horns) and to a lesser extent the contralateral lumbar spinal cord (Fig. 4f; Supplemental Fig. 1f). Additionally, inclusions were observed in the ipsilateral thoracic and cervical spinal cords of these mice (Fig. 4d, e; Supplemental Fig. 1d, e). Thus, in these asymptomatic mice there was evidence that an entity capable of inducing pathologic misfolding of G85R-SOD1:YFP protein had begun to spread rostrally in the spinal cord.

In symptomatic mice that were 2 months p.i., there were abundant G85R-SOD1:YFP inclusions in the ipsilateral DRG and to a lesser extent in the contralateral ganglia (Fig. 3e, f). In these animals, inclusions were much more abundant in the lumbar cord, observed on both the ipsilateral and contralateral sides, and readily detected in the neuropil of the ipsilateral and contralateral thoracic cord (Fig. 5c–f). Additionally, in the symptomatic mice, inclusions were now abundantly observed in the ipsilateral cervical cord (Fig. 5a, b). In animals that had reached end-stage (both hind limbs paralyzed) both the ipsilateral and contralateral DRG had numerous G85R-SOD1:YFP inclusions (Fig. 3g, h) and the spinal cords of these animals showed widespread and abundant inclusion pathology, in both sides of the cord and at all levels (Fig. 5g–l). Collectively, these findings demonstrate the appearance of misfolded G85R-SOD1:YFP in structures distal to the site of injection well before symptoms appear and that both the sensory and motor nerves appear to be able to mediate the propagation of misfolded protein.

To quantify the spread of pathology in the spinal cord, we captured images from multiple sections from each region of the cord from at least three animals per timepoint and then used ImageJ to highlight aggregates, which were much more fluorescent than diffusely distributed G85R-SOD1: YFP protein. The entire spinal cord was then outlined and the % area occupied by inclusions within in each section was calculated and averaged among the similar levels of cord for each cohort of animals (1, 2 months asymptomatic, 2 months symptomatic, and paralyzed). These quantified data demonstrate that the delayed appearance of misfolded G85R-SOD1:YFP protein in mice receiving a single sciatic nerve injection of inducing inoculum (Fig. 6a). At 1 month p.i., there was essentially no inclusion pathology in the spinal cord (Fig. 6a). Between 1 and 2 months of age, the burden of inclusion pathology varied. In animals in which disease symptoms had not yet appeared, there was significant inclusion pathology in both the ipsilateral and contralateral lumbar cord, but sparse pathology elsewhere (Fig. 6a). In animals that were developing weakness in the injected limb, the level of inclusion pathology was greater, with a still greater level of pathology in end-stage animals, in which both hind limbs were paralyzed (Fig. 6a). Thus, the data indicate an insidious spread of misfolded G85R-SOD1:YFP that propagates rostrally up the

spinal cord prior to clinical evidence of disease. Aggregate load increased rather dramatically in the interval between the first sign of limb weakness and end-stage paralysis.

We also investigated how this spread of inclusion pathology correlated with glial activation. Using thresholding methods similar to those used for G85R-SOD1-YFP quantification, we observed an increase in GFAP immunoreactivity in the lumbar spinal cord as the mice developed paralysis (Fig. 6b; Supplemental Fig. 2). By comparison, the abundance of GFAP immunoreactivity in more rostral regions of the cord was much lower (Fig. 6b). By comparing the quantification results between inclusion pathology and glial activation (Fig. 6a, b), there was an obvious relationship between the two, with both appearing to accumulate at similar stages of the disease and at similar levels of the cord. Taking our analysis a step further, we also quantified the ChAT-positive motor neurons throughout the cord and found a similar progression of neuronal loss. In the lumbar spinal cord there was a significant reduction (~35 %) of motor neurons in the mice injected with G93A → G85R-SOD1: YFP homogenate in the sciatic nerve at 1 and 2 months p.i. when compared to the control mice that were injected with asymptomatic, heterozygous G85R-SOD1: YFP homogenate (Fig. 6c). The loss of motor neurons in the lumbar cord continued as mice became paralyzed, reaching close to a 65 % loss at end-stage (Fig. 6c). Although we also observed a significant reduction of motor neurons in the thoracic cord at 2 months p.i., and at end-stage, there was no change detected at any timepoint in the cervical cord (Fig. 6c). Together, the results from these quantitative analyses describe a gradient of pathology that is most severe in lumbar spinal cord with lesser degrees of severity more rostrally.

Trans-synaptic spread of inclusion pathology

Rodents lack the direct synaptic connections between upper and lower motor neurons, but the potential exists that misfolded SOD1 could propagate trans-synaptically to the brain through either interneurons or sensory neuron pathways. At 1 month p.i, we could find no inclusion pathology in the brain (Fig. 7a–d). At 2 months p.i., the asymptomatic mice displayed G85R-SOD1:YFP inclusions in the reticular formation and lateral vestibular nucleus of the brainstem, and in the red nucleus, located in the mesencephalon (Fig. 7e–g). The inclusions in these structures were fairly sparse and appeared mainly in the cell body with some also appearing within the neuropil. The symptomatic mice at this timepoint displayed an increased number of inclusions within the reticular formation, but in the lateral vestibular nucleus and red nucleus, the number of inclusions was similar to that of the asymptomatic 2-month p.i. mice (Fig. 7i–k). In addition to these structures, we also observed a small number of inclusions in the periaqueductal gray (PAG) and the motor-related layers of the superior colliculus (Fig. 7l). In fully paralyzed animals at the end-stage of disease, we observed abundant G85R-SOD1:YFP inclusion pathology in these same five neuroanatomical structures; the reticular formation, lateral vestibular nucleus, red nucleus, PAG, and superior colliculus (Fig. 7m–p; Table 2). The brain pathology in these animals was largely confined to these structures with almost no inclusion pathology observed in the forebrain, including the motor cortex.

Discussion

It has long been recognized that the symptoms of ALS seem to spread from one muscle group to another along anatomically connected pathways [5, 20, 21]. Determining what mediates this spread has been elusive. Our study, using the G85R-SOD1:YFP mouse model, provides the first evidence that misfolded protein can mediate the spreading symptoms of ALS. Our data show that misfolded forms of the G85R-SOD1:YFP fusion protein accumulate in tissue prior to the onset of symptoms with an explosive accumulation of inclusion pathology as mice develop the paralytic symptoms at the end-stage of disease. Crucially, no disease symptoms appear in G85R-SOD1:YFP mice injected with spinal homogenates from asymptomatic mice expressing the same fusion protein. Clearly, our study cannot establish that misfolded SOD1 mediates the spread of symptoms in human sporadic ALS or ALS caused by mutations in SOD1. However, the study sets the precedent that a propagating spread of misfolded protein can produce a clinical phenotype that replicates fundamental features of human ALS.

The most important aspect of the model we use here is that injecting inoculum within the sciatic nerve forces the material into a restricted and defined population of neurons that innervate the limb [2, 3]. Following the inoculation of mice with homogenate prepared from G93A → G85R-SOD1: YFP mice unilaterally within the sciatic nerve, we first observed inclusion pathology in the ipsilateral DRG at 1 month p.i. The sciatic nerve is a mixed peripheral nerve, containing predominantly sensory fibers. Therefore, the deposition in the DRG can be explained by retrograde transport from the point of inoculation. At 2 months p.i. in the animals that were asymptomatic, the inclusion pathology first appeared in the lumbar spinal cord, in both the ventral and dorsal regions of the cord. This could be explained by either retrograde spread from the point of inoculation to the ventral motor neurons in laminae IX and/or anterograde spread from the DRG to the dorsal horn. Additionally, these animals displayed sparse inclusions in the contralateral DRG, which can only be explained by retrograde transport from the dorsal columns, which although not abundant, did contain inclusions. In the symptomatic mice, the amount of G85R-SOD1:YFP inclusion pathology increased in both the ipsilateral and contralateral DRG. Together, these data indicate the ability for the G85R-SOD1:YFP aggregate seeds to be transported along the axons in the retrograde direction and, potentially, out to the dorsal horn in the anterograde direction. We did not, however, detect any inclusion pathology in the gastrocnemius muscle at any stage in the disease, suggesting either the lack of anterograde transport from the injection site to the muscle, or the inability for the muscle to accumulate G85R-SOD1:YFP inclusion pathology (Supplementary Fig. 3). Although it is possible that the inducing factor could be transported along the axolemma surface in a cell-to-cell manner, we have observed no G85R-SOD1:YFP pathology along the length of the sciatic nerve at any timepoint examined (data not shown).

ALS is almost completely characterized by motor dysfunction, while sensory abnormalities have been infrequently reported [13, 27]. Although we did not test for any sensory impairments in our mice, the inclusion pathology observed in the DRG and dorsal horn of the spinal cord indicates involvement of the sensory system in our paradigm. Previous studies have documented the accumulation of misfolded SOD1 in sensory structures, and the

degeneration of DRG neurons and sensory axons were observed in mouse models of SOD1 [8, 11, 26]. Therefore, although sensory structures do not appear to be directly involved in the pathogenesis of ALS, based on the lack of a detectable sensory impairment, our data suggest that sensory neurons may serve as conduits for the spreading of misfolded protein conformations.

As indicated above, the G85R-SOD1:YFP pathology was not observed in the spinal cord until 2 months p.i., and in the asymptomatic mice the pathology was mainly restricted to the lumbar region. Importantly, when pathology was observed, it was clear the normal diffuse distribution of G85R-SOD1:YFP in asymptomatic mice had been disturbed. Thus, the appearance of pathology is not the result of some slow accumulation of the inoculated aggregates in neuronal populations, but rather represents the templated conversion of the G85R-SOD1:YFP by a mobile seed. Additionally, the induction and accumulation of SOD1 inclusions were accompanied by gliosis and motor neuron loss that appeared to spread in an identical spatiotemporal manner as the inclusion pathology. Whatever the nature of the "seed", it propagates insidiously rostrally from the lumbar cord and trans-synaptically to the brain before symptoms develop.

Interestingly, in asymptomatic mice at 2 months p.i., although very little G85R-SOD1:YFP pathology was observed in the cervical spinal cord in these animals, we detected inclusions in the reticular formation, lateral vestibular nucleus and red nucleus (Table 2). These structures were also observed to accumulate the infectious prion protein at preclinical timepoints following sciatic nerve inoculation and was attributed to retrograde transport from the ventral motor neurons to these three populations of neurons via the reticulospinal, vestibulospinal, and rubrospinal descending motor tracts, respectively [2, 3]. The lack of pathology in the cervical cord and neuronal populations surrounding these structures strongly implicates neuroanatomical spread as the mechanism utilized to reach these locations, rather than a cell-to-cell, diffusive mechanism of propagation. Additionally, at end-stage when the G85R-SOD1: YFP pathology accumulated in these 3 neuronal populations, we began to detect inclusions in the motor-related layers of the superior colliculus and the periaqueductal gray. The deposition of G85R-SOD1:YFP inclusions in the superior colliculus is most likely due to retrograde transport via the tectospinal tract. Neurons in the intermediate and deep layers of the superior colliculus are known to project to the cervical spinal cord [15], which is in line with our data as the pathology was observed in these structures following deposition in the cervical cord. The pathology observed in the periaqueductal gray can be also be attributed to retrograde transport from the spinal cord, as tracer studies have demonstrated that these neurons project to both cervical and lumbar regions of the cord [16]. Taken together, it appears that in our paradigm, a seed that propagates G85R-SOD1:YFP misfolding is retrogradely transported via trans-synaptic transport from the spinal cord via multiple descending motor pathways and thereby affecting multiple brain regions.

Although our data suggest neuroanatomical spread of the SOD1 seeding factor via several descending motor pathways, it is intriguing that we did not observe any pathology in the motor cortex, which would be indicative of transport from the motor neurons in the lumbar spinal cord via the corticospinal tract. This pathway was one of the four descending

pathways suggested to be utilized in prion transport to the brain upon injection in the sciatic nerve [2, 3]. A lack of G85R-SOD1:YFP expression in these neurons cannot explain the lack of deposition in this region as YFP fluorescence is seen fairly uniformly throughout the brain and observed in neurons in layer 5 of the motor cortex (Supplemental Fig. 4). One possibility is that the disease course in spinal cord was too rapid and that there was insufficient time for the SOD1 seeds to reach this area and/or induce G85R-SOD1:YFP aggregation to levels visible by fluorescence microscopy. Another possibility is that this neuronal population is resistant to the accumulation of G85R-SOD1:YFP aggregation due to some unknown cellular factors or possibly to lower expression of the transgene in these cells when compared to other locations within the CNS. We note that the original report describing paralyzed homozygous G85R-SOD1:YFP mice did not mention pathology in brain [28], and we have not observed cortical inclusion pathology in any paralyzed G85R-SOD1:YFP mice we have analyzed (data not shown). Assuming that the lack of G85R-SOD1:YFP pathology in the motor cortex signals a lack of upper motor neuron defects, then it seems that dysfunction of the lower motor neurons is sufficient to mimic the paralytic symptoms of ALS in mice.

It is unlikely that axonal transport alone can account for the widespread distribution of G85R-SOD1:YFP pathology observed throughout the spinal cord at the end-stage of disease. Most of the G85R-SOD1:YFP inclusions observed in this induced model are located in the neuropil, where it is difficult to define cellular identity because processes from neurons, astrocytes, microglia, and oligodendrocytes co-mingle. It is very likely that cell-to-cell spread is also occurring within spinal axis of these mice. Such cell-to-cell spread could be trans-synaptic spread by interneurons or by other mechanisms in other cell types. Multiple studies have indicated the potential for exogenous SOD1 to be taken up by macropinocytosis or transported between cells through tunneling nanotubes or within exosomes [9, 10]. Our data clearly indicate trans-synaptic spread can occur but do not rule out other mechanisms of misfolded G85R-SOD1:YFP propagation.

Taken together, this study provides strong evidence that the G85R-SOD1:YFP fusion protein can produce propagating seeds of misfolded protein that spread from a localized point of entry to engulf the entire spinal axis. We also uncover the potential for the sensory system to act as a potential conduit for propagating misfolded proteins. Although we do not presently understand why the G85R-SOD1: YFP model is uniquely permissive to developing motor neuron disease after exposure to tissue preparations containing misfolded SOD1, this model provides a unique opportunity to probe mechanisms of disease spread along significant neuroanatomical distances. This model also provides a superior system to test whether a particular therapeutic approach may halt the progression of disease by slowing the spread of a proteotoxin; and to determine the optimal therapeutic window for such treatments.

Supplementary Material

Refer to Web version on PubMed Central for supplementary material.

Acknowledgments

We thank Drs. Todd Golde, Benoit Giasson, and Anthony Kincaid for helpful advice over the course of these experiments. This work was supported by a grant from the National Institutes of Neurological Disease and Stoke (1R01NS092788-01), the Packard Center for ALS Research at Johns Hopkins University and the Milton Safenowitz Post-Doctoral Fellowship for ALS Research awarded by the ALS Association.

References

1. Ayers J, Fromholt S, Koch M, DeBosier A, McMahon B, Xu G, Borchelt DR. Experimental transmissibility of mutant SOD1 motor neuron disease. Acta Neuropathol. 2014; 128:791–803. [PubMed: 25262000]
2. Ayers J, Kincaid AE, Bartz JC. Prion strain targeting independent of strain-specific neuronal tropism. J Virol. 2009; 83:81–87. [PubMed: 18971281]
3. Bartz JC, Kincaid AE, Bessen RA. Retrograde transport of transmissible mink encephalopathy within descending motor tracts. J Virol. 2002; 76:5759–5768. [PubMed: 11992004]
4. Borchelt DR, Lee MK, Slunt HS, Guarnieri M, Xu ZS, Wong PC, Brown RH, Price DL, Sisodia SS, Cleveland DW. Superoxide dismutase 1 with mutations linked to familial amyotrophic lateral sclerosis possesses significant activity. Proc Natl Acad Sci USA. 1994; 91:8292–8296. [PubMed: 8058797]
5. Brooks BR. The role of axonal transport in neurodegenerative disease spread: a meta-analysis of experimental and clinical poliomyelitis compares with amyotrophic lateral sclerosis. Can J Neurol Sci. 1991; 18:435–438. [PubMed: 1718581]
6. Bruijn LI, Houseweart MK, Kato S, Anderson KL, Anderson SD, Ohama E, Reaume AG, Scott RW, Cleveland DW. Aggregation and motor neuron toxicity of an ALS-linked SOD1 mutant independent from wild-type SOD1. Science. 1998; 281:1851–1854. [PubMed: 9743498]
7. Clavaguera F, Bolmont T, Crowther RA, Abramowski D, Frank S, Probst A, Fraser G, Stalder AK, Beibel M, Staufenbiel M, Jucker M, Goedert M, Tolnay M. Transmission and spreading of tauopathy in transgenic mouse brain. Nat Cell Biol. 2009; 11:909–913. [PubMed: 19503072]
8. Fischer LR, Li Y, Asress SA, Jones DP, Glass JD. Absence of SOD1 leads to oxidative stress in peripheral nerve and causes a progressive distal motor axonopathy. Exp Neurol. 2011
9. Grad LI, Guest WC, Yanai A, Pokrishevsky E, O'Neill MA, Gibbs E, Semenchenko V, Yousefi M, Wishart DS, Plotkin SS, Cashman NR. Intermolecular transmission of superoxide dismutase 1 misfolding in living cells. Proc Natl Acad Sci USA. 2011
10. Grad LI, Yerbury JJ, Turner BJ, Guest WC, Pokrishevsky E, O'Neill MA, Yanai A, Silverman JM, Zeineddine R, Corcoran L, Kumita JR, Luheshi LM, Yousefi M, Coleman BM, Hill AF, Plotkin SS, Mackenzie IR, Cashman NR. Intercellular propagated misfolding of wild-type Cu/Zn superoxide dismutase occurs via exosome-dependent and -independent mechanisms. Proc Natl Acad Sci USA. 2014; 111:3620–3625. [PubMed: 24550511]
11. Guo YS, Wu DX, Wu HR, Wu SY, Yang C, Li B, Bu H, Zhang YS, Li CY. Sensory involvement in the SOD1-G93A mouse model of amyotrophic lateral sclerosis. Exp Mol Med. 2009; 41:140–150. [PubMed: 19293633]
12. Gurney ME, Pu H, Chiu AY, Dal Canto MC, Polchow CY, Alexander DD, Caliendo J, Hentati A, Kwon YW, Deng HX. Motor neuron degeneration in mice that express a human Cu, Zn superoxide dismutase mutation. Science. 1994; 264:1772–1775. [PubMed: 8209258]
13. Isaacs JD, Dean AF, Shaw CE, Al-Chalabi A, Mills KR, Leigh PN. Amyotrophic lateral sclerosis with sensory neuropathy: part of a multisystem disorder? J Neurol Neurosurg Psychiatry. 2007; 78:750–753. [PubMed: 17575021]
14. Jucker M, Walker LC. Self-propagation of pathogenic protein aggregates in neurodegenerative diseases. Nature. 2013; 501:45–51. [PubMed: 24005412]
15. Leong SK, Shieh JY, Wong WC. Localizing spinal-cord-projecting neurons in adult albino rats. J Comp Neurol. 1984; 228:1–17. [PubMed: 6434598]
16. Mantyh PW, Peschanski M. Spinal projections from the periaqueductal grey and dorsal raphe in the rat, cat and monkey. Neuroscience. 1982; 7:2769–2776. [PubMed: 7155351]

17. Münch C, O'Brien J, Bertolotti A. Prion-like propagation of mutant superoxide dismutase-1 misfolding in neuronal cells. Proc Natl Acad Sci USA. 2011; 108:3548–3553. [PubMed: 21321227]
18. Peelaerts W, Bousset L, Van der Perren A, Moskalyuk A, Pulizzi R, Giugliano M, van den Haute C, Melki R, Baekelandt V. α-Synuclein strains cause distinct synucleinopathies after local and systemic administration. Nature. 2015; 522:340–344. [PubMed: 26061766]
19. Prudencio M, Hart PJ, Borchelt DR, Andersen PM. Variation in aggregation propensities among ALS-associated variants of SOD1: correlation to human disease. Hum Mol Genet. 2009; 18:3217–3226. [PubMed: 19483195]
20. Ravits J, Paul P, Jorg C. Focality of upper and lower motor neuron degeneration at the clinical onset of ALS. Neurology. 2007; 68:1571–1575. [PubMed: 17485643]
21. Ravits JM, La Spada AR. ALS motor phenotype heterogeneity, focality, and spread: deconstructing motor neuron degeneration. Neurology. 2009; 73:805–811. [PubMed: 19738176]
22. Rosen DR, Siddique T, Patterson D, Figlewicz DA, Sapp P, Hentati A, Donaldson D, Goto J, O'Regan JP, Deng HX. Mutations in Cu/Zn superoxide dismutase gene are associated with familial amyotrophic lateral sclerosis. Nature. 1993; 362:59–62. [PubMed: 8446170]
23. Sacino AN, Brooks M, Thomas MA, McKinney AB, Lee S, Regenhardt RW, McGarvey NH, Ayers J, Notterpek L, Borchelt DR, Golde TE, Giasson BI. Intramuscular injection of α-synuclein induces CNS α-synuclein pathology and a rapid-onset motor phenotype in transgenic mice. Proc Natl Acad Sci USA. 2014; 111:10732–10737. [PubMed: 25002524]
24. Sacino AN, Thomas MA, Ceballos-Diaz C, Cruz PE, Rosario AM, Lewis J, Giasson BI, Golde TE. Conformational templating of α-synuclein aggregates in neuronal-glial cultures. Mol Neurodegener. 2013; 8:17. [PubMed: 23714769]
25. Sanders DW, Kaufman SK, DeVos SL, Sharma AM, Mirbaha H, Li A, Barker SJ, Foley AC, Thorpe JR, Serpell LC, Miller TM, Grinberg LT, Seeley WW, Diamond MI. Distinct tau prion strains propagate in cells and mice and define different tauopathies. Neuron. 2014; 82:1271–1288. [PubMed: 24857020]
26. Sábado J, Casanovas A, Tarabal O, Hereu M, Piedrafita L, Calderó J, Esquerda JE. Accumulation of misfolded SOD1 in dorsal root ganglion degenerating proprioceptive sensory neurons of transgenic mice with amyotrophic lateral sclerosis. BioMed Res Int. 2014; 2014:1–13.
27. Theys PA, Peeters E, Robberecht W. Evolution of motor and sensory deficits in amyotrophic lateral sclerosis estimated by neurophysiological techniques. J Neurol. 1999; 246:438–442. [PubMed: 10431767]
28. Wang J, Farr GW, Zeiss CJ, Rodriguez-Gil DJ, Wilson JH, Furtak K, Rutkowski DT, Kaufman RJ, Ruse CI, Yates JR, Perrin S, Feany MB, Horwich AL. Progressive aggregation despite chaperone associations of a mutant SOD1-YFP in transgenic mice that develop ALS. Proc Natl Acad Sci USA. 2009; 106:1392–1397. [PubMed: 19171884]
29. Wang J, Slunt H, Gonzales V, Fromholt D, Coonfield M, Copeland NG, Jenkins NA, Borchelt DR. Copper-binding-site-null SOD1 causes ALS in transgenic mice: aggregates of non-native SOD1 delineate a common feature. Hum Mol Genet. 2003; 12:2753–2764. [PubMed: 12966034]
30. Watts JC, Condello C, Stöhr J, Oehler A, Lee J, Dearmond SJ, Lannfelt L, Ingelsson M, Giles K, Prusiner SB. Serial propagation of distinct strains of Aβ prions from Alzheimer's disease patients. Proc Natl Acad Sci USA. 2014; 111:10323–10328. [PubMed: 24982139]

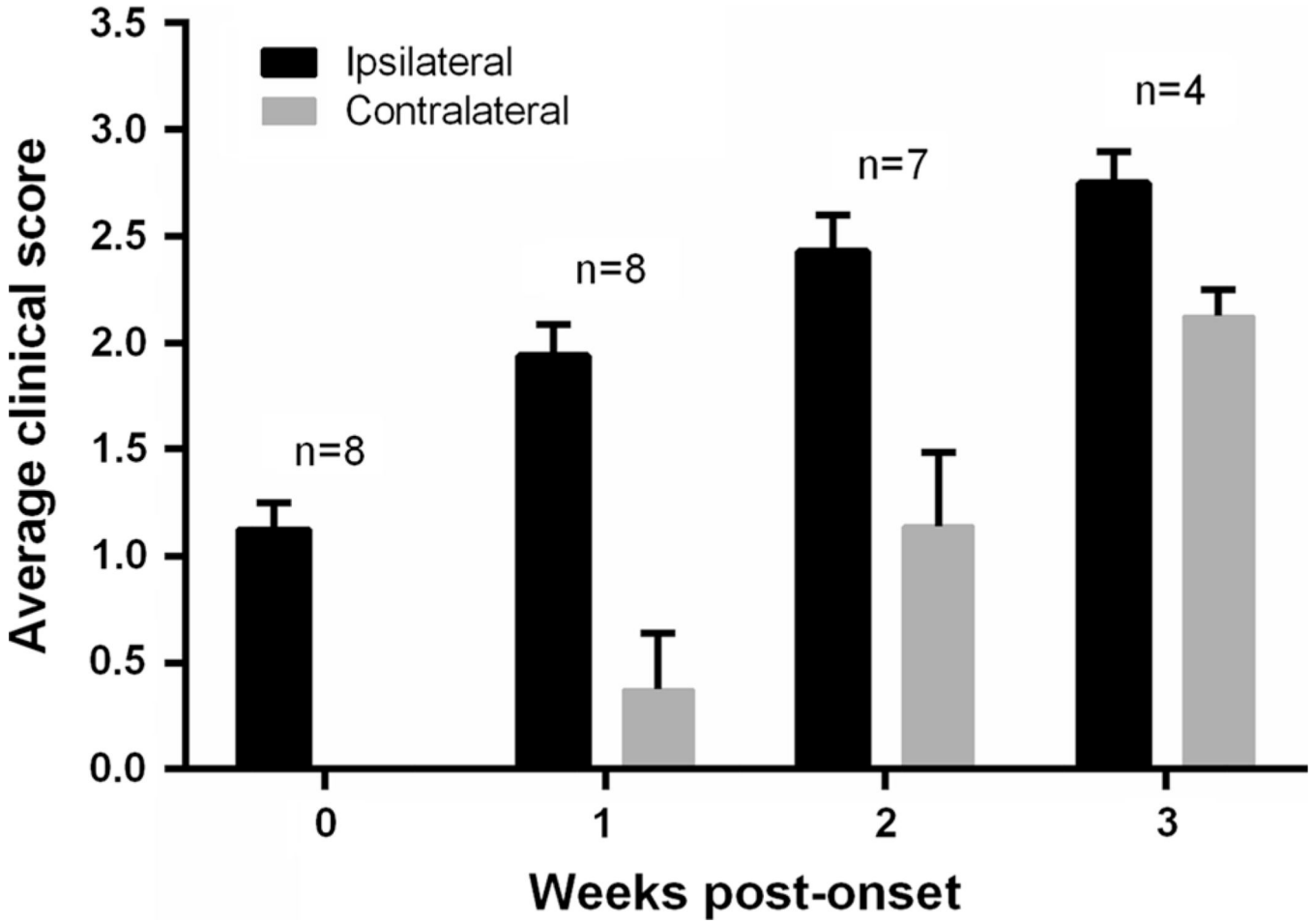

Fig. 1.

Differential onset of paralysis in ipsilateral versus contralateral hind limbs. Hind limb weakness and paralysis was assessed for each limb based on a scoring system from 0 (no weakness) to 3 (disease end-stage), as described in the “Methods”. Hind limb weakness was first observed in the ipsilateral limb in all of the injected animals that reached end-stage and then appeared in the contralateral limb 1–2 weeks later. Only seven mice survived to 2 weeks post-symptom onset and only four survived to 3 weeks post-onset before reaching the end-stage of disease

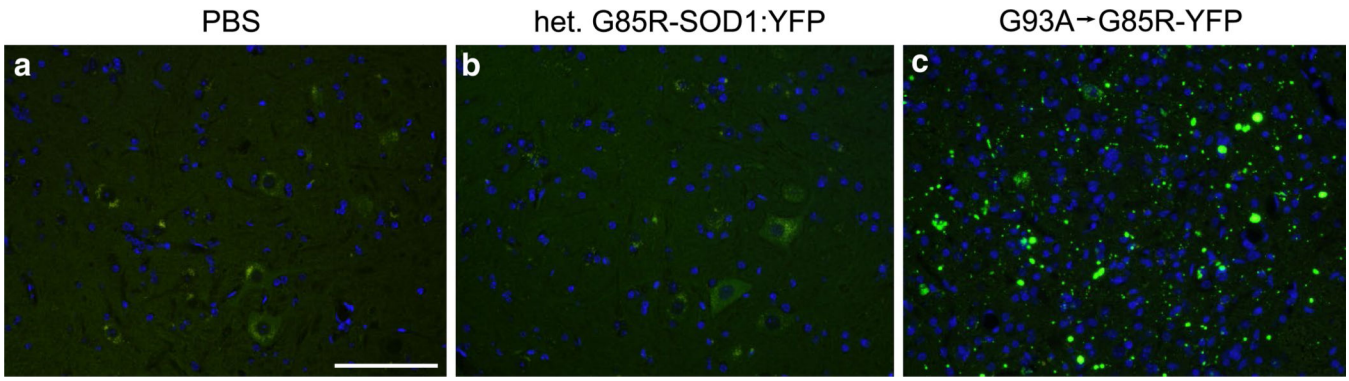

Fig. 2.

Induction of inclusion pathology in G85R-SOD1:YFP mice injected with G93A → G85R-SOD1:YFP spinal cord homogenate. G85R-SOD1:YFP mice were injected unilaterally in their sciatic nerve with either PBS (**a**), homogenate from an asymptomatic heterozygous G85R-SOD1:YFP mouse (**b**), or homogenate from a mouse paralyzed by injection of G93A → G85R-SOD1:YFP second passage homogenates (**c**). The PBS-injected mice (*n* = 3) were harvested at 12.6 months p.i. and mice injected with homogenate from the asymptomatic G85R-SOD1:YFP mouse (*n* = 5) were harvested at 8.5 months p.i.; neither cohort displayed G85R-SOD1:YFP inclusion pathology in any level of their spinal cord. Abundant YFP inclusion pathology was observed in end-stage mice (~3 months) injected with the second passage G93A → G85R-SOD1:YFP homogenates (*n* = 8). *Scale bars* 100 μm

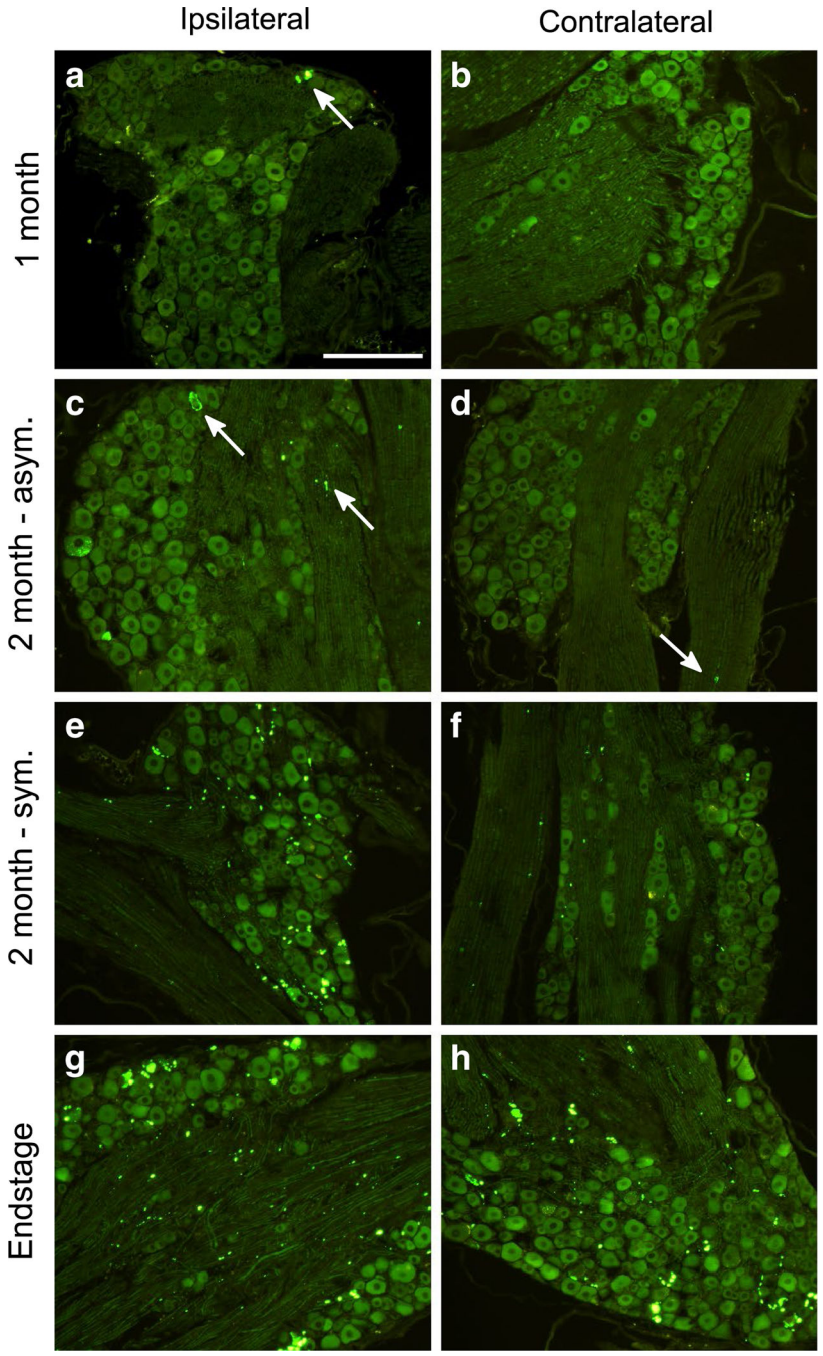

Fig. 3.

Accumulation of SOD1:YFP pathology over time in the DRG of sciatic nerve injected animals. The L3, L4, and L5 DRG were dissected from mice at various timepoints p.i. (*n* = 3–4 per timepoint) from both the ipsilateral (*left column*) and contralateral (*right column*) sides of the spinal column, and processed for paraffin embedding. Following deparaffinization, direct YFP fluorescence was imaged. G85R-SOD1:YFP inclusion pathology was first observed at 1 month p.i. (**a**, **b**) in the ipsilateral DRG (indicated by *arrow*) and grew more abundant in both the asymptomatic (**c**, **d**) and symptomatic (**e**, **f**)

mice at 2 months p.i. **g**, **h** The mice at the end-stage of disease had abundant pathology in their DRG both ipsilateral and contralateral to the side of inoculation. Inclusions indicated by *arrows*. *Scale bars* 200 μm

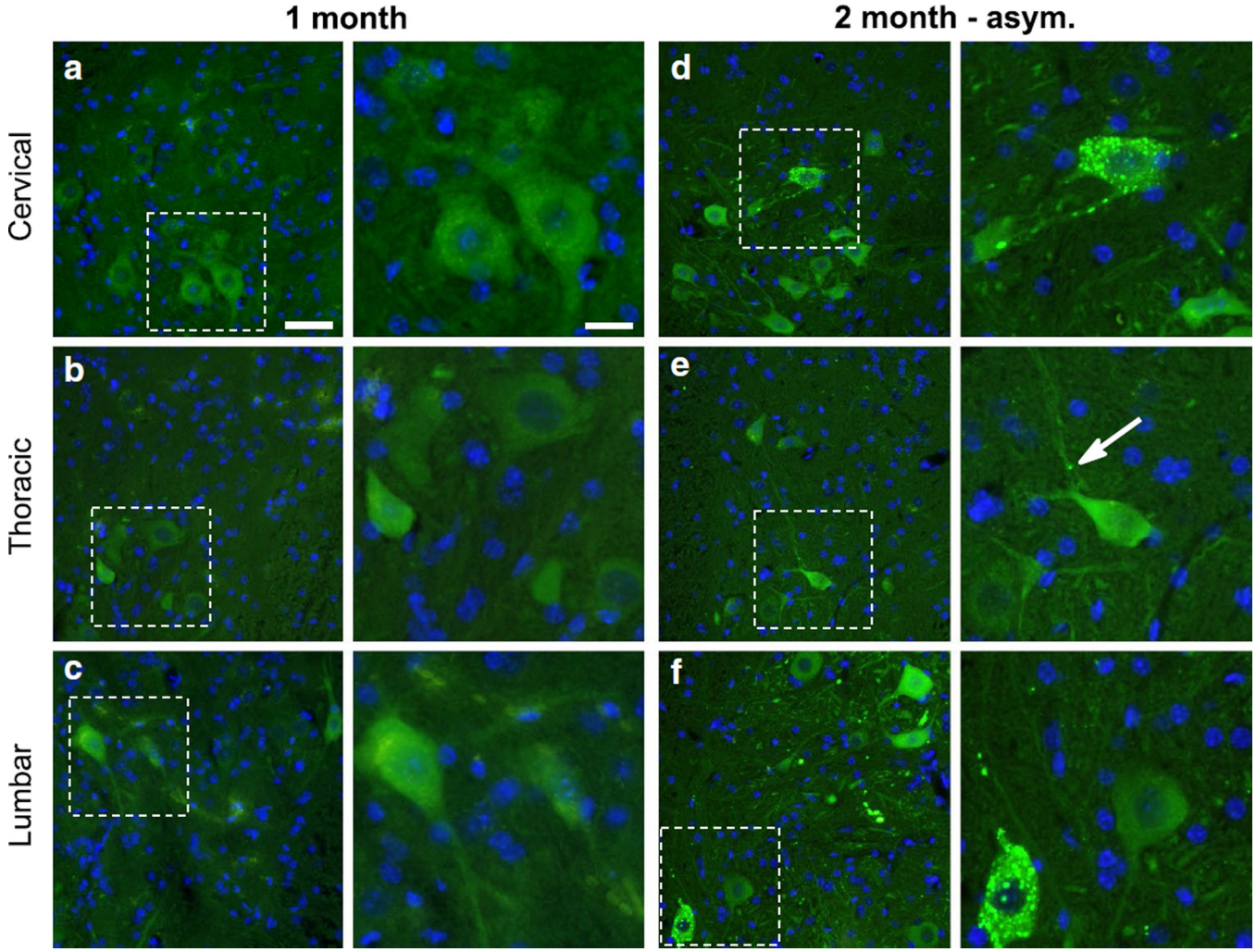

Fig. 4.

Initial deposition of G85R-SOD1:YFP inclusions in the lumbar spinal cord. The spinal cords from mice at various timepoints (n = 3–4 per timepoint) were harvested and processed for paraffin embedding while careful consideration was made to ensure correct orientation of the tissue. **a**–**c** No G85R-SOD1:YFP pathology was observed in any level of the cord at 1 month p.i. (low magnification in *left panels*; high magnification in *right panels*). In asymptomatic mice at 2 months p.i., inclusions were infrequent in thoracic and cervical cord (**d**, **e**), but relatively numerous in the lumbar cord (**f**). Inclusions indicated by *arrows*. *Scale bars* 50 μm, low magnification; 25 μm, high magnification

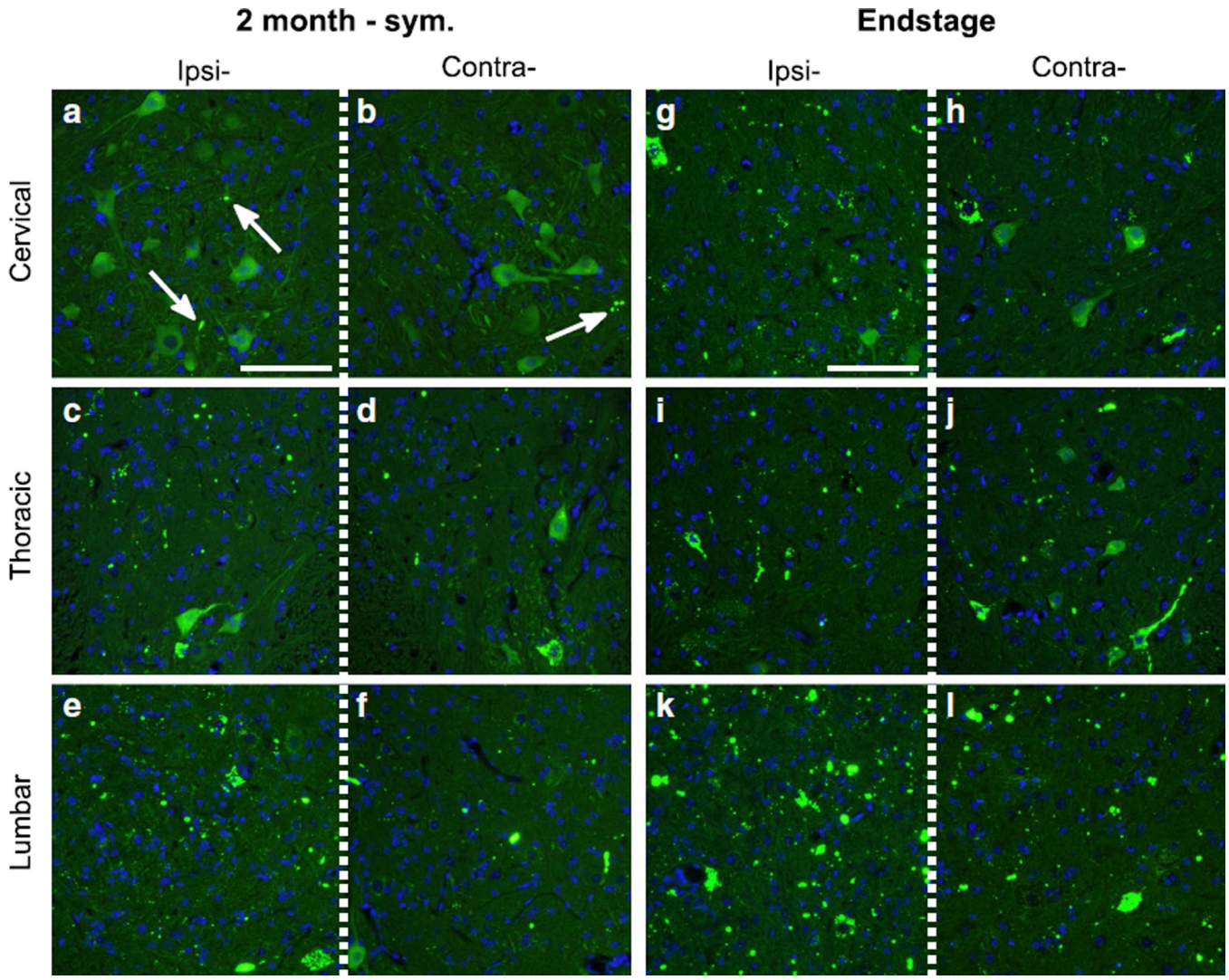

Fig. 5.

Progressive spread of G85R-SOD1:YFP inclusion pathology rostrally throughout the spinal cord. Direct fluorescence of the DRG revealed abundant YFP inclusion pathology on the ipsilateral side with fewer inclusions observed in the contralateral DRG. **a**–**f** In the spinal cords of symptomatic mice at 2 months p.i., the inclusions increased in abundance in all levels of the ipsilateral spinal cord and began appearing on the contralateral side of the thoracic and cervical spinal cord. **g**–**l** The mice at the end-stage of disease had abundant pathology in all levels of the spinal cord, both on the ipsilateral and contralateral side. Inclusions indicated by *arrows*. *Scale bars* 200 μm

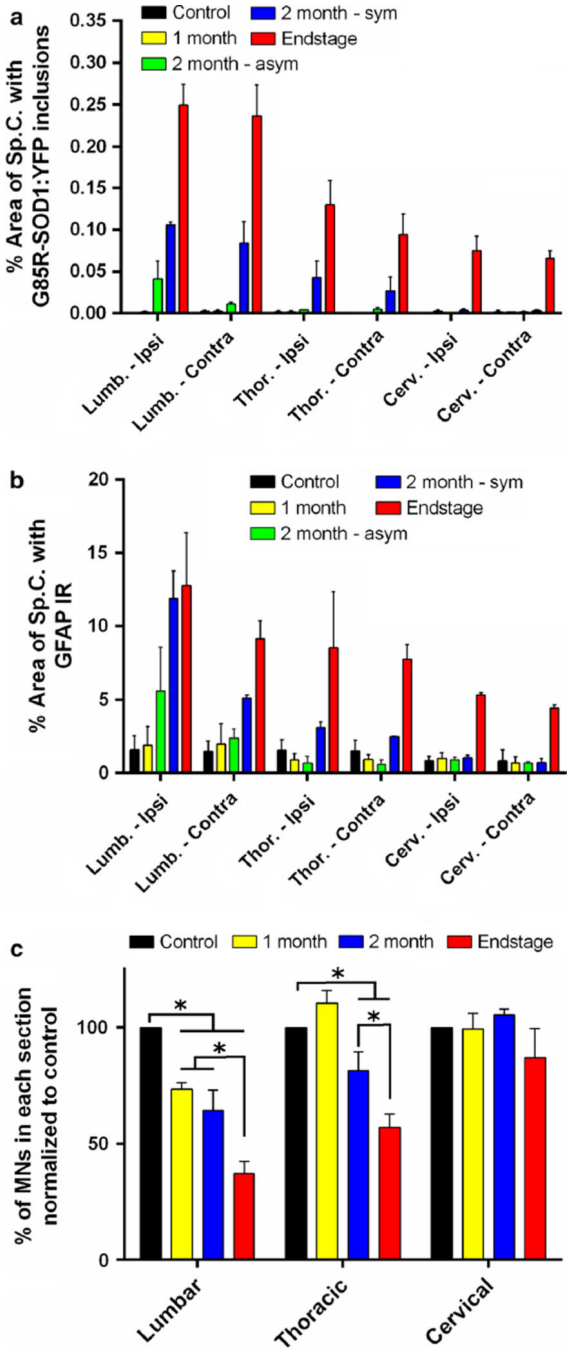

Fig. 6.

Quantification of spinal cord pathology demonstrating a caudal to rostral gradient of pathology. The percent area of the spinal cord covered by G85R-SOD1:YFP inclusions (**a**) or GFAP immunoreactivity (**b**) increased over time moving from caudal to rostral. Fluorescent images of various spinal cord segments were captured and the brightness of the G85R-SOD1:YFP inclusions or GFAP immunoreactivity over the background signal allowed thresholding of each image. The percent area covered by the SOD1 inclusions and GFAP-positive astrocytes mirrored one another. In asymptomatic mice at 2 months p.i. these

pathologies were most evident in the lumbar spinal cord. In symptomatic mice at 2 months p.i., inclusions and GFAP-positive astrocytes were evident in the thoracic spinal cord. In end-stage mice, both pathologies were abundant in lumbar and thoracic cord, beginning to take hold in cervical cord. (**c**) There was also a significant reduction in the number of ChAT-positive motor neurons over time in both the lumbar and thoracic regions of the spinal cord when compared to the controls. The control group was mice injected with homogenate from an asymptomatic heterozygous G85R-SOD1:YFP mouse. For all panels, quantification was derived from 3 animals per timepoint and 14 (**a**, **b**) or 28 (**c**) spinal cord sections per animal. ChAT-positive motor neuron counts were totaled for each spinal cord level, averaged per section counted, and normalized to the counts obtained for the controls. Data are presented as mean ± S.E. (*error bars*). Student's *t* test, $*p < 0.05$

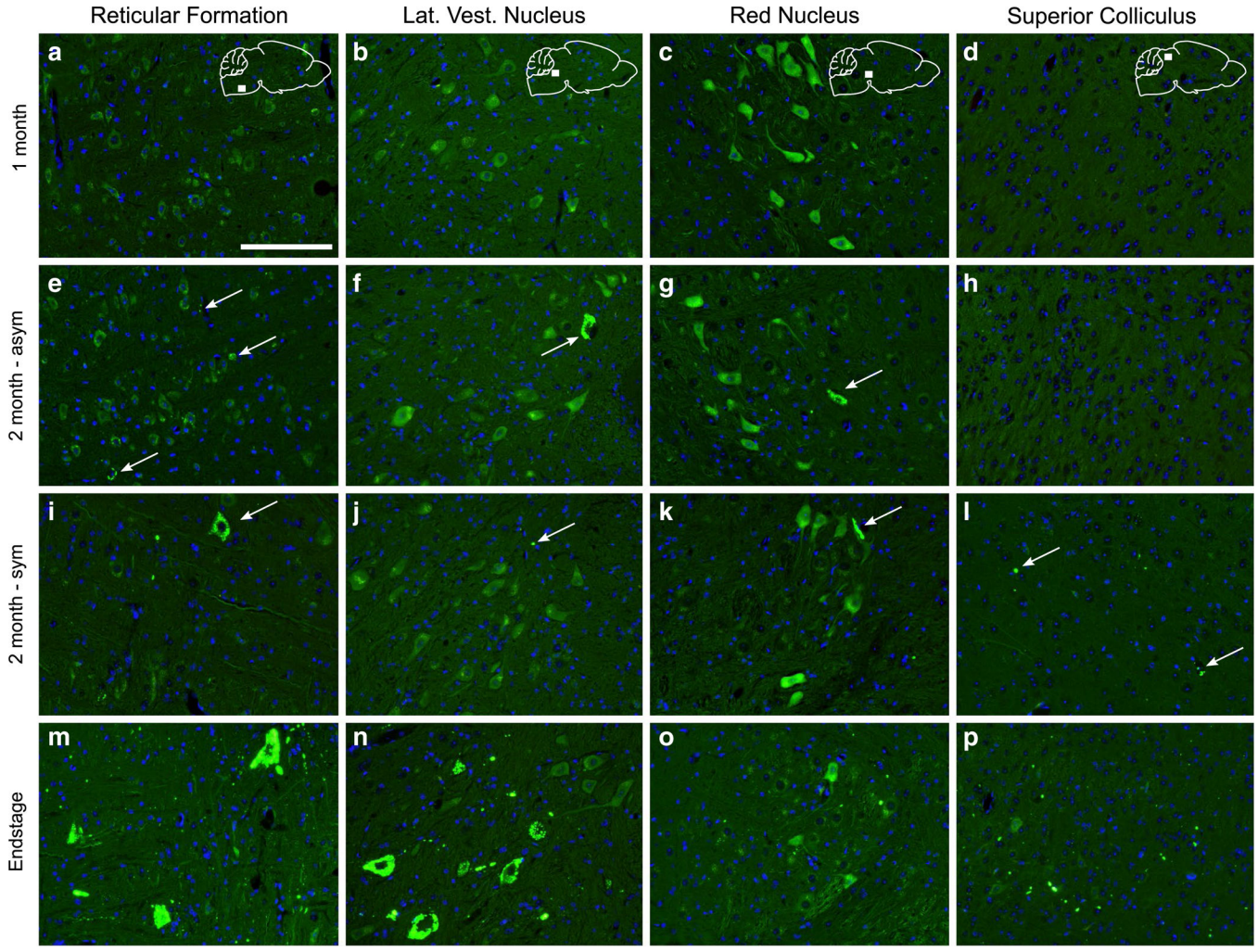

Fig. 7.

Accumulation of YFP inclusion pathology in brain nuclei indicative of trans-synaptic spread of misfolded SOD1. The brain was analyzed at various timepoints p.i. following paraffin embedding and sectioning. **a**–**d** At 1 month p.i. no inclusion pathology was observed throughout the brain. **e**–**h** In the brains of the asymptomatic mice at 2 months p.i., sparse YFP inclusions were detected in the reticular formation, lateral vestibular nucleus, and red nucleus. **i**–**l** In the symptomatic mice at this same timepoint, we also began to observe pathology in the superior colliculus, along with the previously mentioned structures. **m**–**p** By the end-stage of disease, the pathology in these structures had greatly increased in abundance. Inclusions indicated by *arrows*. *Scale bars* 100 μm

Table 1

Data on G85R-SOD1: YFP mice injected with the indicated preparations

	No. paralyzed/no. inoculated	Average (in months) to paralysis	Age of oldest asymptomatic mice (months p.i.)
Uninjected	0/7	n.a.	17.0
Sciatic nerve injected			
Uninjected, asymptomatic G85R-SOD1:YFP hom.	0/5	n.a.	8.5
PBS	0/3	n.a.	12.6
G93A → G85R-SOD1:YFP hom.	8/10	3.0 ± 0.2	8.5

Table 2

Spatiotemporal distribution and abundance of G85R-SOD1: YFP inclusion pathology following sciatic nerve inoculation with G85R-SOD1:YFP homogenate

	1 month	2 month-asym	2 month-sym	End-stage
Spinal cord				
Lumbar	_[a]	++	+++	+++
Thoracic	−	+	++	+++
Cervical	−	+	+	+++
Brain				
Ret. Form.	−	+	++	+++
Lat. Vest. Nuc.	−	+	+	++
Red. Nuc.	−	+	+	++
Periaq. gray	−	−	+	++
Sup. Coll.	−	−	+	++
Mot. Cx.	−	−	−	−

[a] Relative abundance of YFP inclusion pathology

−, none; +, rare; ++, numerous; +++, abundant and widespread